JCTC Journal of Chemical Theory and Computation

Article

pubs.acs.org/JCTC

High On/Off Conductance Switching Ratio via H-Tautomerization in Quinone

Sherif Abdulkader Tawfik,*[,†] X. Y. Cui,*[,‡] S. P. Ringer,[‡] and C. Stampfl[†]

[†]School of Physics, [‡]Australian Centre for Microscopy and Microanalysis, and School of Aerospace, Mechanical and Mechatronic Engineering, The University of Sydney, Sydney, New South Wales 2006, Australia

ABSTRACT: Through first-principles electron transport simulations using the nonequilibrium Green's function formalism together with density functional theory, we show that, upon H-tautomerization, a simple derivative of quinone can act as a molecular switch with high ON/OFF ratio, up to 70 at low bias voltage. This switching behavior is explained by the quantum interference effect, where the positional change of hydrogen atoms causes the energies of the transmission channels to overlap. Our results suggest that this molecule could have potential applications as an effective switching device.

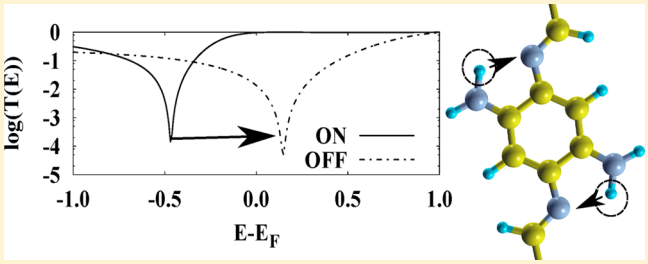

INTRODUCTION

Since the initial proposal of using single molecules as the fundamental building blocks in electronic devices,[1] transport phenomena at the single-molecular level constitute the central properties for conductance switching,[2−4] where quantum interference effects (QIE) play a critical role in the electronic properties of single metal−molecule−metal junctions.[5−7] An ideal switch requires fast and large changes in electronic conductance, i.e., well-defined ON and OFF states, by a gate electrode.[2] Most molecular switches, with some exhibiting high switching ratios (as high as 300 in an optoelectronic switch[8]), are based on dramatic conformational changes in the molecule,[2] which is not compatible with the design of complex devices assembled from single-molecular components.[9,10]

To overcome these drawbacks, a breakthrough in molecular switching was introduced by Liljeroth et al.[10] via hydrogen transfer (H-tautomerization). Using a voltage pulse at the scanning tunneling microscope (STM) tip to induce a change in the orientation of the hydrogen atom pair at the center of naphthalocyanine, observable switching behavior was induced, with a switching ratio of 2 at low temperature. Since H-tautomerization does not radically change the molecular frame, it facilitates ultrafast and reproducible switching.[9−11] Using the nonequilibrium Green's function formalism (NEGF), Prasongkit et al.[12] predicted that H-tautomerization in naphthalocyanine leads to the emergence of well-defined ON and OFF conductance states. Recently, Simpson et al.[13] demonstrated that H-tautomerisation can be realized in quinone derivatives using STM, representing a new class of metal-bound molecular bistable structures. However, the transport behavior in these quinone derivatives has not yet been investigated.

In this work, we complement the novel experimental discovery by Simpson et al.[13] by theoretically analyzing the current−voltage characteristics and studying the QIE, which is underlying the dramatic change in conductivity observed in two H-tautomers of 3,6-diimino-1,4-cyclohexadiene-1,4-diamine (DCD) (the simplest quinone derivative investigated in ref 13), depicted in Figure 1. Our results show that the switching ratio (SR) in DCD, when anchored between two cumulene (carbon chain) electrodes, could be as high as 70 due to a change in the position of the transmission dip upon H-tautomerization from the Para-1 tautomer (OFF state) to the Para-2 tautomer (ON state).

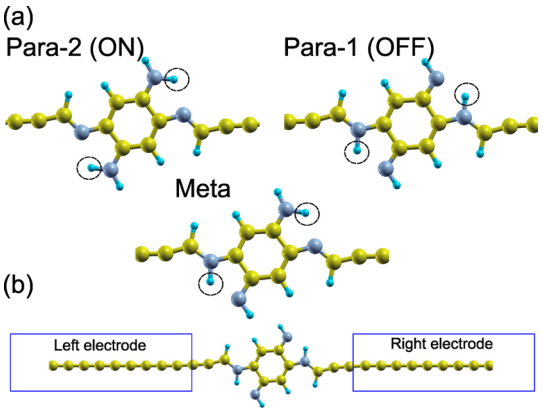

Figure 1. (a) Three isomers of DCD and (b) the setup of the computational system, which shows the two cumulene electrodes and the DCD molecule occupying the scattering region. Yellow spheres denote C atoms, small blue spheres denote H atoms, and dark blue spheres denote N atoms. The dashed circles on the H atoms indicate those that change positions.

MODEL AND COMPUTATIONAL DETAILS

While the DCD considered in ref 13 was adsorbed on a substrate for vertical STM transmission, we focus on the intrinsic transport properties of the isolated DCD molecule in a planar (2D)

Received: May 28, 2015

DOI: 10.1021/acs.jctc.5b00505
J. Chem. Theory Comput. XXXX, XXX, XXX−XXX

form, whereby the electric current flows across the plane of the molecule. This methodology allows us to make predictions about the applicability of the molecule as a potential functional circuit component for possible nanoelectronic applications. We study the transport properties of DCD bonded to two atomic carbon wires (a similar scheme was employed in refs 12 and 14). We use atomic carbon wires, or cumulene, as electrodes because they are considered to be ideal conductive molecular wires.[16,17]

We perform density functional theory (DFT) calculations with the SIESTA code,[18] using the generalized gradient approximation for the exchange-correlation functional as developed by Perdew, Burke, and Ernzerhof (PBE).[19] SIESTA uses basis sets composed of numerical atomic orbitals and approximates the atomic potential in terms of Troullier−Martins norm-conserving pseudopotentials.[20] The auxiliary basis uses a real-space mesh with a kinetic energy cutoff of 200 Ry, and the basis functions are radially confined using an energy shift of 0.005 Ry (see ref 18 for details). The valence states are 2s2p for C and N, 1s for H, and 5d6s for Au. The supercells are created with a large enough vacuum region to prevent interaction due to repeated images. We model the transport of the three DCD isomers shown in Figure 1a by connecting them to cumulene electrodes, as illustrated in Figure 1b.

Regarding the effect of exchange-correlation functional on the results, DFT is known to underestimate the gap between the highest occupied (HOMO) and lowest unoccupied (LUMO) molecular orbitals (HOMO−LUMO gap) and, therefore, typically overestimates the conductance.[12] However, NEGF-DFT calculations with GGA as well as the local density approximation (LDA) have been widely employed.[14,15] More importantly, the QIE that occurs between the HOMO and LUMO derives from the characteristics and symmetry of the molecular orbitals rather than from their precise energetic positions.[21] Therefore, we believe that the present calculations provide good estimates of the switching ratio.

The calculation involves a two-step procedure. First, we perform relaxation of the ionic positions of the scattering structure, while the atomic positions of the other two regions (left and right electrodes) are fixed during the coordinate optimization iterations (the equilibrium C−C bond length between cumulene and DCD is 1.38 Å). Second, we perform transport calculations based on the NEGF method as implemented in the TRANSIESTA code.[22] The double-ζ plus polarization basis set (DZP) is used in the coordinate relaxation step, whereas single-ζ plus polarization is used in the transport calculations. When a molecule is placed between electrodes (Figure 1b), the current I through it as a function of the bias voltage V_{bias} across the device can be estimated using the Landauer−Buttiker formula[23]

$$I(V_{bias}) = \frac{2e}{h}\int_{\infty}^{-\infty} T(E,V_{bias})[f_L(E-\mu_L) - f_R(E-\mu_R)]\,dE \quad (1)$$

where L and R denote left and right electrodes, respectively, $T(E,V_{bias})$ is the transmission function, which is a function of the energy (E), and V_{bias} is the voltage applied across the electrodes. $f_{L/R}$ is the Fermi−Dirac distribution function, and $\mu_{L/R}$ is the electrochemical potential. $T(E,V_{bias})$ is the trace of the square of the transmission amplitude $\mathbf{t}$, and it takes the form

$$T(E,V_{bias}) = \mathrm{Tr}[\mathbf{t}^{\dagger}\mathbf{t}] = \mathrm{Tr}[\Gamma_R G_C \Gamma_L G_C^{\dagger}] \quad (2)$$

where $\Gamma_{R/L}$ is the imaginary part of the self-energy and G_C is Green's function for the contact region.

RESULTS AND DISCUSSION

The calculated current−voltage characteristics (IVC) of the three systems, Para-1, Para-2, and Meta, are shown in Figure 2a,

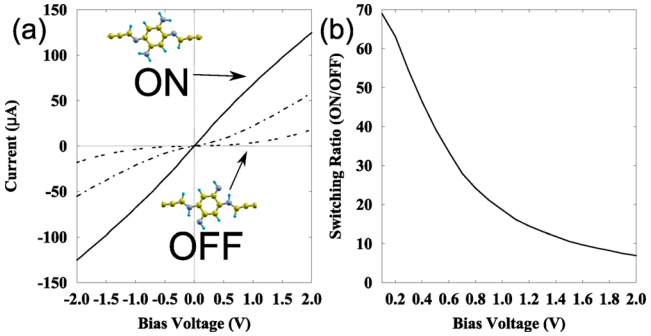

Figure 2. (a) Current−voltage characteristics of the ON, meta, and OFF structures linked to two atomic carbon nanowires and (b) the corresponding ON/OFF switching ratio as a function of bias voltage.

and the switching ratio (SR), defined as $I(V_{bias})_{ON}/I(V_{bias})_{OFF}$ between the ON and OFF states, is shown in Figure 2b. The SR for $V > 0$ starts at a high value ~70 and then falls off as V_{bias} increases, similar to the behavior reported in ref 12. This SR is larger than the SR computed in ref 12 (~40 in the case of cumulene electrodes and ~50 in the case of gold electrodes). Additionally, the computed current values for the ON state have a relatively high range (above 100 μA for V_{bias} = 2.0 V, compared with a maximum of ~60 μA for V_{bias} = 2.0 V in ref 12), corresponding to very large conductance in the ON state that might impart the DCD molecule with practical advantages. These results show that, given that it is possible to induce H-tautomerization in DCD,[13] it can operate as a low-bias molecular switch.

Regarding the IVC of the Meta state, it is intermediate between the IVC of the ON and OFF states, as shown in Figure 2a. Energetically, the Para-2 state (Figure 1a) has the lowest total energy, whereas the Para-1 state is 0.11 eV higher, followed by the Meta state, which is 0.18 eV higher. This situation is similar to gas-phase DFT calculations reported in ref 13, but it is different from DFT calculations of the DCD molecule adsorbed on a Cu(110) slab, where the Meta state is the most energetically favored. With the meta state being the least favorable configuration and its IVC lying in between that of the ON and OFF states for the whole voltage range, we consider only the ON and OFF states hereafter.

The large difference in conductance between the ON and OFF systems can be explained in terms of the transmission function. Figure 3 shows the transmission function of the two states as a function of the bias voltage and electron energy with respect to the Fermi level. The V-shaped lines indicate the boundaries of the bias window, where each line is related to the bias voltage V_{bias} with the equation $E(V_{bias}) = V_{bias}/2$. For a molecular junction, $T(E)$ typically exhibits peaks around the orbital energies, where electrons can resonantly tunnel. The monotonously high conductance of the ON state can be understood from Figure 3, where it can be seen that more of the high-transmission region is included within the bias window as the bias voltage is increased. In the OFF state at V_{bias} = 0 V, the transmission function shows a transmission dip, or antiresonance, due to destructive

DOI: 10.1021/acs.jctc.5b00505
J. Chem. Theory Comput. XXXX, XXX, XXX−XXX

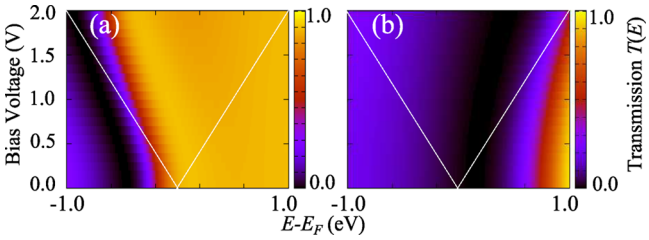

Figure 3. Transmission function, $T(E)$, as a function of energy (relative to Fermi energy) and bias voltage for the (a) ON and (b) OFF states. The white lines represent the bias window.

interference close to the Fermi level. Destructive quantum interference results in the situation where the transmission function of a molecular structure undergoes a dip at certain energies (see ref 24 and references therein) and is a characteristic feature of many nonlinear transport phenomena.[5−7,15,25−31] Figure 4a shows this characteristic transmission dip by displaying

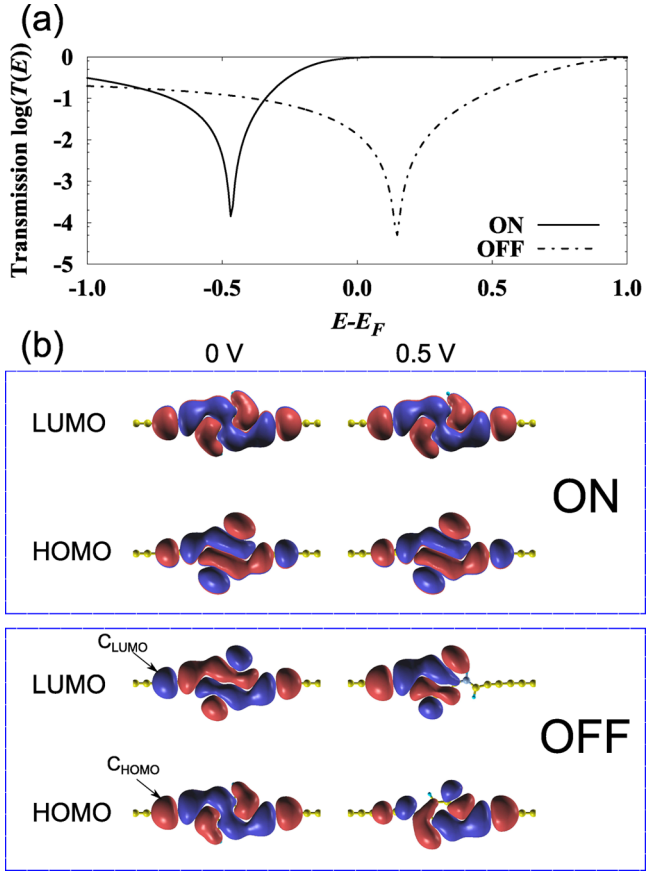

Figure 4. (a) Transmission function $T(E)$ of the ON and OFF states at V_{bias} = 0 V, shown on the logarithmic scale. (b) MPSH isographs at isolevel of the HOMO and LUMO energy levels. In the LUMO wave function of the OFF state at V = 0.5 V, the electron density is almost decoupled from the right electrode. The labels C_{HOMO} and C_{LUMO} refer to the eigenchannel coefficient at the position of the C atom of the electrode, showing that in the OFF state $C_{HOMO} \sim -C_{LUMO}$, whereas in the ON state, $C_{HOMO} \sim C_{LUMO}$.

the transmission functions of the OFF state (as well as a transmission dip in the ON state) on a logarithmic scale. This transmission dip in the OFF state is of the order of 10^{-4}, which is very low in comparison to the nearly 100% transmission in the ON state at the same energy point (this corresponds to a zero-bias conductance ratio [the ratio between $T(E)$ in the ON and OFF states] of $\sim 10^4$, which is much higher than the value of 431 reported in ref 12). The the ON state also has a transmission dip at −0.461 eV. However, because the transmission dip of the OFF state is close to the Fermi level (at E = 0.148 eV), the current resulting from this transmission (by integrating across the energy as in eq 1) is very low in comparison with that resulting from the transmission function of the ON state. Therefore, H-tautomerization has resulted in a shift of the interference further away to the left, i.e., to lower energy, thus placing the high-transmission region (the yellow region Figure 3) within the bias window.

The transmission dip in the OFF states in Figure 4a can be explained by the occurrence of destructive interference, where the electron injected from the left electrode can hop through the DCD molecule via two possible quantum-interfering paths, namely, the molecular projected self-consistent Hamiltonian (MPSH) HOMO and LUMO, because they are near-degenerate (the calculated energy of the HOMO is −0.032 eV, whereas that of the LUMO is 0.042 eV). In contrast, in the ON state, the calculated HOMO energy is −0.195 eV, whereas that of the LUMO is 0.513 eV. This relatively large spacing between the HOMO and LUMO states in the ON state means that if the electron is in one of the two states, it will require a large amount of energy (~0.71 eV) in order to hop from HOMO to LUMO. Therefore, the QIE does not occur in the ON state around the Fermi level. Interestingly, the increase in the bias voltage from 0 to 0.5 V, as shown in Figure 4b, does not seem to alter the electronic character of the MPSH orbitals of the ON state significantly. In contrast, the rise in the bias voltage induces significant change in the electronic character of the OFF state. When the bias voltage reaches 0.5 V, for the LUMO the scattering region becomes very weakly coupled to the right electrode (Figure 4b), reducing the conductivity across that channel.

The MPSH orbitals in Figure 4b, evaluated using the Inelastica code,[32] show the evolution of the two main transmission orbitals, LUMO and HOMO, in both the ON and OFF states under bias voltage V = 0 and 0.5 V. We resort to analyzing the LUMO−HOMO because of their usefulness in understanding the switching behavior in organic molecules.[33] The LUMO and HOMO in the ON state exhibit strong π conjugation between the DCD molecule and the electrodes. Note that there is an interesting difference between the electronic characteristics of the HOMO and LUMO in the ON and OFF states: the HOMO of the ON state appears to be almost similar to the LUMO of the OFF state, except that the signs of the orbital at the points labeled C_{HOMO} and C_{LUMO} are opposite but almost equal in magnitude. These labels are the coefficients of the MPSH orbitals at C atoms connected to the electrodes, and, as will be shown below, their opposite signs lead to the suppression of transmission in the OFF state.

To understand how this observation correlates with the presence of a transmission dip at a small energy point above the Fermi level in the OFF state (0.148 eV), we utilize the representation of Green's function in terms of the expansion coefficients of the MPSH orbitals given by[34,35]

$$G_{ba}(E_F) \approx \frac{C^*_{b\mathrm{HOMO}} C_{a\mathrm{HOMO}}}{E_F - \epsilon_{\mathrm{HOMO}} \pm i\eta} + \frac{C^*_{b\mathrm{LUMO}} C_{a\mathrm{LUMO}}}{E_F - \epsilon_{\mathrm{LUMO}} \pm i\eta} \qquad (3)$$

where a and b denote atoms in the system, $C_{a/b\mathrm{HOMO}}$ is the coefficient of the MPSH orbital of energy the HOMO at site a/b,

DOI: 10.1021/acs.jctc.5b00505
J. Chem. Theory Comput. XXXX, XXX, XXX−XXX

$C_{a/b\mathrm{LUMO}}$ is that for the LUMO, and $\epsilon_{\mathrm{HOMO/LUMO}}$ is the energy of the HOMO/LUMO. Considering the transmission dip of the OFF state, which occurs at 0.148 eV, we make the substitutions E_F = 0.148 eV, ϵ_{HOMO} = −0.032 eV, and ϵ_{LUMO} = 0.042 eV into eq 3. The result is that the denominators of the two terms in eq 3 are close, whereas the numerators of the two terms have opposite signs ($C^*_{b\mathrm{HOMO}}C_{a\mathrm{HOMO}} \approx -C^*_{b\mathrm{LUMO}}C_{a\mathrm{LUMO}}$, given that $\pm i\eta$ is negligible). This clearly makes $G_{ba}(E_F) \approx 0$, thus resulting in the transmission dip of the OFF state. As for the transmission dip in the ON state, it cannot be explained in terms of eq 3 because there are no near-degenerate orbitals around the position of the dip at E_F = −0.461 eV. Note that the dip in the ON state does not affect the transmission because it is positioned far from the Fermi energy.

In conclusion, through first-principles calculations, we have demonstrated that H-tautomerization of the DCD molecule between two cumulene electrodes leads to the emergence of distinctive ON and OFF states, where a large switching ratio as high as 70 is attainable at a low bias voltage. This behavior can be explained by the quantum interference effect. Thus, our results show that cumulene−DCD−cumulene can function as a quantum interferometer, where transmission can be switched reversibly by changing the positions of the two H atoms while retaining the original framework of the molecule. Therefore, DCD could possibly be utilized as an effective H-tautomerization induced switch in modular design in all-carbon molecular circuits.

AUTHOR INFORMATION

Corresponding Authors

*(S.A.T.) E-mail: tawfik@physics.usyd.edu.au.

*(X.Y.C.) E-mail: carl.cui@sydney.edu.au.

Funding

This research was undertaken with the assistance of resources from the National Computational Infrastructure (NCI), which is supported by the Australian Government.

Notes

The authors declare no competing financial interest.

REFERENCES

(1) Aviram, A.; Ratner, M. A. Molecular Rectifiers. *Chem. Phys. Lett.* **1974**, *29*, 277−283.

(2) Sun, L.; Diaz-Fernandez, Y. A.; Gschneidtner, T. A.; Westerlund, F.; Lara-Avila, S.; Moth-Poulsen, K. Single-Molecule Electronics: from Chemecal Design to Functional Devices. *Chem. Soc. Rev.* **2014**, *43*, 7378−7411.

(3) Jia, C.; Guo, X. Molecule-Electrode Interfaces in Molecular Electronic Devices. *Chem. Soc. Rev.* **2013**, *42*, 5642−5660.

(4) Aradhya, S. V.; Venkataraman, L. Single-Molecule Junctions Beyond Electronic Transport. *Nat. Nanotechnol.* **2013**, *8*, 399−410.

(5) Baer, R.; Neuhauser, D. Phase Coherent Electronics: A Molecular Switch Based on Quantum Inter- ference. *J. Am. Chem. Soc.* **2002**, *124*, 4200−4201.

(6) Hsu, L.-Y.; Li, E. Y.; Rabitz, H. Single-Molecule Electric Revolving Door. *Nano Lett.* **2013**, *13*, 5020−5025.

(7) Guedon, C. M.; Valkenier, H.; Markussen, T.; Thygesen, K. S.; Hummelen, J. C.; van der Molen, S. J. Observation of Quantum Interference in Molecular Charge Transport. *Nat. Nanotechnol.* **2012**, *7*, 305−309.

(8) Jia, C.; Wang, J.; Yao, C.; Cao, Y.; Zhong, Y.; Liu, Z.; Liu, Z.; Guo, X. Conductance Switching and Mechanisms in Single-Molecule Junctions. *Angew. Chem., Int. Ed.* **2013**, *52*, 8666−8670.

(9) Andrews, D. Q.; Solomon, G. C.; van Duyne, R. P.; Ratner, M. A. Single Molecule Electronics: Increasing Dynamic Range and Switching Speed Using Cross-Conjugated Species. *J. Am. Chem. Soc.* **2008**, *130*, 17309−17319.

(10) Liljeroth, P.; Repp, J.; Meyer, G. Current-Induced Hydrogen Tautomerization and Conductance Switching of Naphthalocyanine Molecules. *Science* **2007**, *317*, 1203−1206.

(11) Kong, H.; Sun, Q.; Wang, L.; Tan, Q.; Zhang, C.; Sheng, K.; Xu, W. Atomic-Scale Investigation on the Facilitation and Inhibition of Guanine Tautomerization at Au(111) Surface. *ACS Nano* **2014**, *8*, 1804−1808.

(12) Prasongkit, J.; Grigoriev, A.; Ahuja, R.; Wendin, G. Interference Effects in Phtalocyanine Controlled by H-H Tautomerization: Potential Two-Terminal Unimolecular Electronic Switch. *Phys. Rev. B: Condens. Matter Mater. Phys.* **2011**, *84*, 165437.

(13) Simpson, G. J.; Hogan, S. W. L.; Caffio, M.; Adams, C. J.; Fruchtl, H.; van Mourik, T.; Schaub, R. New Class of Metal Bound Molecular Switches Involving H-Tautomerism. *Nano Lett.* **2014**, *14*, 634−639.

(14) Zhang, Z.; Guo, C.; Kwong, D. J.; Li, J.; Deng, X.; Fan, Z. A Dramatic Odd-Even Oscillating Behavior for the Current Rectification and Negative Differential Resistance in Carbon-Chain-Modified Donor-Acceptor Molecular Devices. *Adv. Funct. Mater.* **2013**, *23*, 2765−2774.

(15) Michoff, M. E. Z.; Castillo, M. E.; Leiva, E. P. A Reversible Molecular Switch Based on the Biphenyl Structure. *J. Phys. Chem. C* **2013**, *117*, 25724−25732.

(16) Beck, W.; Niemer, B.; Wieser, M. Methods for the Synthesis of μHydrocarbon Transition Metal Complexes without MetalMetal Bonds. *Angew. Chem., Int. Ed. Engl.* **1993**, *32*, 923−949.

(17) Lang, N. D.; Avouris, P. Oscillatory Conductance of Carbon-Atom Wires. *Phys. Rev. Lett.* **1998**, *81*, 3515−3518.

(18) Soler, J. M.; Artacho, E.; Gale, J. D.; Garcia, A.; Junquera, J.; Ordejon, P.; Sanchez-Portal, D. The SIESTA Method for Ab Initio Order-N Materials simulation. *J. Phys.: Condens. Matter* **2002**, *14*, 2745.

(19) Perdew, J. P.; Burke, K.; Ernzerhof, M. Generalized Gradient Approximation Made Simple. *Phys. Rev. Lett.* **1996**, *77*, 3865−3868.

(20) Troullier, N.; Martins, J. A Straightforward Method for Generating Soft Transferable Pseudopotentials. *Solid State Commun.* **1990**, *74*, 613−616.

(21) Markussen, T.; Stadler, R.; Thygesen, K. S. The Relation between Structure and Quantum Interference in Single Molecule Junctions. *Nano Lett.* **2010**, *10*, 4260−4265.

(22) Brandbyge, M.; Mozos, J.-L.; Ordejon, P.; Taylor, J.; Stokbro, K. Density-Functional Method For Nonequilibrium Electron Transport. *Phys. Rev. B: Condens. Matter Mater. Phys.* **2002**, *65*, 165401.

(23) Datta, S. *Electronic Transport in Mesoscopic Systems*; Ahmed, H., Pepper, M., Broers, A., Eds.; Cambridge University Press: Cambridge, England, 1995.

(24) Lambert, C. J. Basic Concepts of Quantum Interference and Electron Transport in Single-molecule Electronics. *Chem. Soc. Rev.* **2015**, *44*, 875−888.

(25) Markussen, T.; Schiotz, J.; Thygesen, K. S. Electrochemical Control of Quantum Interference in Anthraquinone-Based Molecular Switches. *J. Chem. Phys.* **2010**, *132*, 224104.

(26) Hansen, T.; Solomon, G. C.; Andrews, D. Q.; Ratner, M. A. Interfering Pathways in Benzene: An Analytical Treatment. *J. Chem. Phys.* **2009**, *131*, 194704.

(27) Aradhya, S. V.; Meisner, J. S.; Krikorian, M.; Ahn, S.; Parameswaran, R.; Steigerwald, M. L.; Nuckolls, C.; Venkataraman, L. Dissecting Contact Mechanics from Quantum Interference in Single-Molecule Junctions of Stilbene Derivatives. *Nano Lett.* **2012**, *12*, 1643−1647.

(28) Fracasso, D.; Valkenier, H.; Hummelen, J. C.; Solomon, G. C.; Chiechi, R. C. Evidence for Quantum Interference in SAMs of Arylethynylene Thiolates in Tunneling Junctions with Eutectic GaIn (EGaIn) Top-Contacts. *J. Am. Chem. Soc.* **2011**, *133*, 9556−9563.

(29) Guedon, C. M.; Valkenier, H.; Markussen, T.; Thygesen, K. S.; Hummelen, J. C.; van der Molen, S. J. Observation of Quantum Interference in Molecular Charge Transport. *Nat. Nanotechnol.* **2012**, *7*, 305−309.

(30) Solomon, G. C.; Andrews, D. Q.; Goldsmith, R. H.; Hansen, T.; Wasielewski, M. R.; Van Duyne, R. P.; Ratner, M. A. Quantum

DOI: 10.1021/acs.jctc.5b00505
J. Chem. Theory Comput. XXXX, XXX, XXX−XXX

Interference in Acyclic Systems: Conductance of Cross-Conjugated Molecules. *J. Am. Chem. Soc.* **2008**, *130*, 17301−17308.
(31) Solomon, G. C.; Andrews, D. Q.; van Duyne, R. P.; Ratner, M. A. When Things Are Not as They Seem: Quantum Interference Turns Molecular Electron Transfer "Rules" Upside Down. *J. Am. Chem. Soc.* **2008**, *130*, 7788−7789.
(32) Paulsson, M.; Brandbyge, M. Transmission Eigenchannels from Nonequilibrium Green's Functions. *Phys. Rev. B: Condens. Matter Mater. Phys.* **2007**, *76*, 115117.
(33) Deng, W.-Q.; Muller, R. P.; Goddard, W. A. Mechanism of the Stoddart-Heath Bistable Rotaxane Molecular Switch. *J. Am. Chem. Soc.* **2004**, *126*, 13562−13563.
(34) Yoshizawa, K.; Tada, T.; Staykov, A. Orbital Views of the Electron Transport in Molecular Devices. *J. Am. Chem. Soc.* **2008**, *130*, 9406−9413.
(35) Tada, T.; Yoshizawa, K. Quantum Transport Effects in Nanosized Graphite Sheets. *ChemPhysChem* **2002**, *3*, 1035−1037.

DOI: 10.1021/acs.jctc.5b00505
J. Chem. Theory Comput. XXXX, XXX, XXX−XXX